

1
2 **Repeated inversion and collapse on the Late Cretaceous – Cenozoic northern Vøring**
3 **Basin, Norway**

4
5 Lundin, Erik, R.¹, Doré, Anthony, G.², Rønning, K.³, & Kyrkjebø, R.¹

6
7 1) Statoil Research Centre, PO Box 2470, 7005 Trondheim, NORWAY

8 2) Statoil UK Ltd., One Kingdom Street, London W2 6BD, UK.

9 3) Statoil ASA, PO Box 40, Medkila, 9481 Harstad, NORWAY

10

11 **Abstract**

12
13 The Norwegian Atlantic margin, although frequently described as passive, has seen several
14 significant and highly variable deformation events prior to and after early Cenozoic break-up.
15 This chronology is strongly exemplified in the northern Vøring Basin, where deformation
16 resulted in significant vertical motions, including deep erosion and sediment reworking.

17
18 Post-break-up compressional deformation is well documented in the NE Atlantic margins,
19 and is represented in the north Vøring Basin by the Vema and Naglfar Domes. A prominent
20 Maastrichtian-Paleocene pre-breakup phase of compression inverted the northern
21 prolongation of the latest Turonian Vigrid Syncline. This syncline was the fairway for the c 1
22 km thick Santonian-Campanian Nise sandstone, shed from NE Greenland and/or the western
23 Barents Sea margin. The inversion focused on the Vigrid Syncline axis, forming an anticline
24 here referred to as the Vema-Nyk Anticline. The anticline may have been a major trap, but
25 was breached by erosion prior to collapse due to Late Paleocene extension. The remnant
26 eastern half of the anticline is the Nyk High. The associated flanking syncline, the Någrind
27 Syncline, also remains preserved. The collapsed side of the anticline is the Hel Graben,
28 which itself was inverted in the Middle Miocene time forming the Naglfar and Vema Domes.

29
30 More speculatively, the development of the Vigrid Syncline and its bounding structural highs
31 the Gjallar Ridge and Utgard High may also represent folds, marking the onset of
32 compressional buckling in the mid-Norwegian – NE Greenland rift system.

33
34 The repeated compressional deformation, as well as the extensional collapse, was focused on
35 the area subjected to Early Cretaceous hyperextension. Compressional buckling under
36 relatively low stress levels is proposed to have been due to significant lithosphere weakening
37 caused by the hyperextension, whereby both high attenuation of the crystalline crust and
38 serpentinization of the upper mantle contribute to the weakening. The Late Cenozoic
39 compression postdated the hyperextension by c 110 m.y., which, suggests that the weakening
40 is long-lived and that lithosphere has not been strengthened significantly through time.

41
42
43 Key words: NE Atlantic, serpentinization, inversion, hyperextension, folding, compression,
44 collapse

45

46 **Introduction**

47

48 The area of study lies in the northern Vøring Basin and is part of a Cretaceous-Cenozoic
49 basin system along the NE Atlantic passive margin (e.g. Doré et al., 1999). Structural
50 features in the mid-Norwegian rifted margin (Fig. 1) were named by Blystad et al (1995).

51

52 The mid-Norwegian margin has a long history of episodic rifting, spanning between the
53 Carboniferous and Early Eocene break-up, a duration of c 250 m.y. During this long period
54 the extensional stress field rotated significantly, resulting in oblique overprinting of older by
55 younger rifts events (Fig. 2). This is spectacularly displayed by the Early Cretaceous rift
56 which “beheaded” the Late Jurassic rift system (e.g. Lundin & Doré, 1997, Doré et al, 1999;
57 Roberts et al, 1999), and by the oblique line of Paleocene rifting and Early Eocene break-up
58 versus the trend of the Cretaceous rift system. As a consequence of the oblique break-up, the
59 hyperextended Early Cretaceous basin chain that once spanned from the West Orphan Basin
60 to the Bjørnøya Basin (Lundin & Doré, 2011) is today fragmented into abandoned
61 hyperextended basin elements on conjugate North and NE Atlantic margins.

62

63 A suite of mid- to Late Cenozoic compressional features within the NE Atlantic rifted
64 margins, most prominent between the northern Vøring Basin and the northern Rockall
65 Trough, has been well documented in the literature (e.g. Doré et al, 2008, Johnson et al.
66 2005, Tuitt et al. 2010). A less well-documented suite of broad folds representing Late
67 Cretaceous compressional shortening has been described in the Vøring Basin (Brekke, 2000;
68 Lundin & Doré, 2011). Both sets of structures are predominantly located within the
69 fragmented Early Cretaceous basin elements and a causal relationship with lithospheric
70 weakening due to hyperextension has been proposed (Lundin & Doré, 2011). In this paper
71 we show how the complex structure of the northern Vøring Basin was influenced by Early
72 Cretaceous hyperextension, setting the stage for multi-phase inversion before and after break-
73 up, and how the same area was further imprinted by collapse immediately prior to continental
74 separation.

75

76 Our usage of the term “hyperextension” refers to a situation whereby the crust has been
77 sufficiently thinned by extension to cause coupling between the lower and upper crust
78 (Perez-Gussinye & Reston, 2006; Sutra & Manatschal, 2012), in turn permitting faults to
79 penetrate the entire crust, and thereby hydrate the upper mantle.

80

81 **Structural features of the north Vøring Basin**

82

83 The Vigrid Syncline is a latest Turonian (Brekke et al, 2001) through Paleocene sub-basin in
84 the outer Vøring Basin, bounded by the Gjallar Ridge highs to the west, the Utgard High and
85 Fles Fault Zone to the east, and the Rym Fault Zone to the north (Figs. 2 & 3). The Någrind
86 Syncline is a Maastrichtian to Paleocene sub-basin bounded to the north by the Bivrost
87 Lineament, to the east by the Utgard High, and to the west by the Nyk High. The Nyk High is
88 a truncated fault block that has been interpreted as an eroded footwall to the more enigmatic
89 Hel Graben (e.g. Lundin & Doré, 1997; Walker et al., 1997; Ren et al, 2003). All of these
90 authors have assumed that these features were formed by extension of approximately

91 Paleocene age - an episode that heralded Early Eocene break-up and spreading in the adjacent
92 North Atlantic.

93

94 The southern boundary to Hel Graben is overprinted by a north-trending anticline, the Vema
95 Dome (Fig 4), which is interpreted to have formed by Middle Miocene compression (e.g.
96 Lundin & Doré, 2002; Doré et al, 2008). In this paper we show that the Vema Dome first rose
97 in Late Maastrichtian to Late Paleocene time (Figs. 5 and 6), collapsed in Paleocene time
98 (Figs. 7, and 8), and became domed into its current shape in Middle Miocene time (Figs. 5
99 and 6). The sedimentary fill of the Hel Graben was inverted to form the Naglfar Dome (Fig.
100 8), which is loosely constrained to be a Middle Miocene inversion structure. The south and
101 southwest boundaries to Hel Graben are defined by the Rym Fault Zone, which here is
102 considered to be a flexure or faulted flexure. The northwest side of Hel Graben is defined by
103 the Vøring Escarpment, constituting the boundary against the Vøring Marginal High. The
104 escarpment has been interpreted to mark a palaeo-coastline in the inner basalt flows
105 manifested as a sharp cliff line (e.g. Planke et al., 1999) but is also a faulted structural break
106 (Brekke, 2000). The marginal high remains an enigmatic feature and is generally assumed to
107 be highly intruded transitional crust covered by Late Paleocene plateau basalts associated
108 with break-up (Skogseid & Eldholm, 1988).

109

110 The Vigrid Syncline spans the Vøring Basin from the Gjallar Ridge in the west to the Fles
111 Fault Complex in the east. Flexure of the Vigrid Syncline was initiated in Late Turonian time
112 (Brekke et al, 2001). The Late Turonian to Paleocene succession onlaps westward against
113 the eastern flank of the Gjallar Ridge, in places to a single point of pinch-out. The western
114 side of the Gjallar Ridge is marked by numerous fault blocks, bound by west-throwing
115 normal faults (e.g. Lundin & Dore, 1997; Ren et al, 2003; Gernigon et al, 2004). These faults
116 have been interpreted to be of Late Cretaceous to Paleocene age (op. cit.). We return to the
117 age of the Gjallar Ridge faulting in the discussion.

118

119 **Late Cretaceous inversion**

120

121 The mid-Norwegian margin (Fig. 1) contains a thick succession of Cretaceous strata, which
122 to date generally has been interpreted as a post-rift succession to Late Jurassic-Early
123 Cretaceous rifting (e.g. Doré et al, 1999). The Early Cretaceous Vøring Basin was reshaped
124 into broad folds in Cenomanian-Turonian time (Brekke 2000; Brekke et al., 2001; Lundin &
125 Doré, 2011). Apart from the sources mentioned above, this reshaping of the basin in the
126 early Late Cretaceous has been little remarked upon in the literature, where it is tacitly
127 assumed that most of the Cretaceous was represented by passive subsidence and basin infill.
128 However, like Brekke (2000), we point out that the general fold-like geometry of major
129 structures such as the Någrind Syncline (Fig. 9a), the Vigrid Syncline (Fig. 9b) and its
130 bounding anticlines suggest regional (albeit mild) compression. Notably, the syncline is not
131 underlain by a rifted terrain, but rather by a relatively uniformly thick Cretaceous succession.
132 Thus, the syncline is clearly not a thermal response to rifting. Even the use of the “syncline”
133 nomenclature (Blystad et al. 1995) probably represents an unconscious acknowledgement
134 that the local geometries do not fit a standard extensional pattern. Stratal patterns, such as
135 the onlap of Cenomanian-Paleocene reflectors on to the eastern flank of the Gjallar Ridge
136 (e.g. Lundin & Doré, 1997; Ren et al. 2003; Gernigon et al, 2004) support deformation of
137 this age, specifically the rise of the Gjallar Ridge as a bounding anticline of the Vigrid

138 Syncline. Similar evidence for Late Cretaceous deformation is observed at the Utrøst Ridge
139 in the outer Lofoten margin. Seismic data reveal onlap of Late Cretaceous strata against the
140 eastern side of the Utrøst Ridge (e.g. profile C-C', Blystad et al, 1995) and the timing is
141 constrained to the Late Cenomanian by IKU borehole 6711/04 U01 (Hansen et al, 1992).
142 Originally Brekke (2000) interpreted the timing of the onset of the Vigrid Syncline to the
143 Cenomanian, but later (Brekke et al, 2001) revised this to latest Turonian. The discrepancy
144 between this Latest Turonian date on the northwestern flank of the Vigrid Syncline and the
145 Cenomanian date from the IKU borehole may relate to dating uncertainty, or could indicate
146 regional variability in onset of the deformation.

147

148 The Vigrid Syncline resembles basins formed by lithospheric folding (Cloetingh & Burov,
149 2010). Folding of the basin started c 40-60 m.y. after the Early Cretaceous hyperextension.
150 The wavelength of the Vigrid Syncline fold is in the order of 80 km, The Rås and Træn
151 Basins east of the Utgard High/Fles Fault Complex probably represent another synclinal fold,
152 with the Utgard High and Fles Fault Complex marking the intervening and subsequently
153 collapsed anticline.

154

155 The Någrind Syncline can be viewed as the eastern remnant of a wider inverted syncline
156 (palaeo-Vigrid Syncline) that initially spanned from the Utgard High to the western side of
157 Hel Graben. This development is illustrated by a transect (Fig. 9a) between the Gjallar Ridge
158 (6704/12-1), Vema Dome (6706/11-1), Nyk High (6707/10-1), and Utgard High (6605/7-2).
159 This section and seismic data reveal that the Santonian-Early Campanian Nise Formation, an
160 over 1000 m thick sequence (in the former syncline axis) of clean deep water sandstones
161 (Kittilsen et al, 1999) characterized by a distinctive "stripy" seismic response, was deposited
162 in an unstructured saucer-shaped basin. Based on the isochore thickness of the Nise Fm and
163 on seismic facies relationships, the axis of a palaeo-Vigrid Syncline extended approximately
164 through the Vema Dome-Nyk High area. There is a general westward thickening of the Nise
165 Fm, from the Utgard High through the Någrind Syncline to the Nyk High. The Nise Fm and
166 older sequences are folded in the Någrind Syncline and are truncated along the Nyk High
167 fault system (Fig. 7). By implication, deformation forming both the Någrind Syncline and the
168 Vema-Nyk uplift postdate Nise Formation deposition.

169

170 Based on heavy mineral and zircon analyses (e.g. Morton & Grant, 1998; Morton et al, 2005)
171 and analysis of regional unconformities (e.g. Hamann et al, 2005; Tsikalas et al, 2005), the
172 Nise Formation's provenance lay in NE Greenland. The offshore Danmarkshavn Ridge,
173 which was deeply eroded in the Late Cretaceous, is a strong candidate for this provenance.
174 However, a 100 Ma zircon population in the Nise Fm (Morton et al, 2005) cannot easily be
175 tied to NE Greenland but could stem from magmatism in the Svalbard- northern Barents Sea-
176 Amerasia Basin (so-called High Arctic LIP) (e.g. Maher, 2001, Shipilov & Karyakin 2011)).
177 The Svalbard archipelago is also characterized by a major Late Cretaceous erosional
178 unconformity (e.g. Steel & Worsley 1984; Maher, 2001). The influx of voluminous clean
179 sands to the Vøring Basin took place during a period of globally high sea level (Haq et al,
180 1988) and is suggestive of active tectonics. We infer that the Nise Formation deep-water
181 turbidites were deposited south-southeastward from NE Greenland and the northwestern
182 Barents Sea into a gentle palaeo-Vigrid Syncline that spanned the Vøring Basin from north to
183 south. The southern part of the palaeo-syncline is still intact and is represented by the Vigrid
184 Syncline, while the northern part was split by uplift of the Vema-Nyk Anticline.

185

186 The Vema-Nyk Anticline is an informal name we use to indicate the latest Cretaceous uplift
187 that occurred in this area. In a later section we show that this rise was domal in nature, began

188 in the Maastrichtian and continued into the Paleocene. A Maastrichtian isochore map also
189 suggests Maastrichtian onset for rise of the Vema-Nyk Anticline and folding of the Någrind
190 Syncline (Fig. 10). This deformation is considered a clear compressional episode that
191 preceded break-up.
192

193 **Paleocene pre-breakup faulting**

194
195 Pre-breakup extension, beginning in the latest Cretaceous but mainly of Paleocene age, and
196 major marginal magmatism of mainly Paleocene to Early Eocene age have been well
197 documented in the literature (e.g. Doré et al, 1999, Brekke 2000, Skogseid et al. 2000, Ren et
198 al. 2003). In the northern Vøring Basin normal faulting of this age has been documented on
199 the Nyk and Utgard Highs, and thin-skinned faulting has been described in detail on the
200 Gjallar Ridge (Ren et al., 2003). According to the latter authors, the extensional activity was
201 protracted and took place from 85 to 55 Ma, ie essentially spanning the Campanian to
202 Paleocene interval. Such a long period of crustal extension spanning a considerable portion
203 of the Late Cretaceous appears at odds with the idea of mild regional compression causing
204 the inversion of the Vigrid Syncline. However, lines presented by Ren et al. suggest to us
205 that the pre-Paleocene faulting was limited in scope, perhaps representing or including
206 gravitational accommodation on the bounding anticlines as the Vigrid Syncline infilled and
207 subsided. Some expansion against these faults is in places observed between Ren et al's
208 interpreted Campanian reflectors. However, most significantly, all of the reflectors assigned
209 to the Campanian and Maastrichtian are themselves strongly offset by the normal faulting.
210 The faults are truncated abruptly at the Top Cretaceous which in this area is an erosional
211 surface overlain by thin Paleocene sediments, usually Upper Paleocene. These observations
212 suggest that the principal phase of normal faulting occurred in either the latest Cretaceous, or
213 more probably in the Paleocene.
214

215 Strikingly, the most intense pre-breakup faulting occurs on the anticlinal crests – the Nyk
216 High, the Utgard High, the Gjallar Ridge, and the Utrøst Ridge, suggesting that the Late
217 Cretaceous anticlines were unstable and provided a locus for later (mainly Paleocene)
218 extension.

219 **Evolution of the Nyk High, Hel Graben and Vema Dome**

220
221 The Hel Graben was defined seismically by Skogseid & Eldholm (1989) and later named by
222 Blystad et al. (1995) who pointed out that the thick basin fill was of disputed age, ranging
223 from Campanian to Paleocene. The larger Hel Graben area, including the bordering Nyk
224 High, Vema Dome and Rym Fault Zone structures (Fig. 1), has several enigmatic features
225 that require explanation. These include: 1) the pre-collapse Vema-Nyk Anticline, 2) the
226 collapsed western flank of the anticline into Hel Graben, and 3) renewed Middle Miocene
227 doming of the Vema and Naglfar Domes (e.g. Lundin & Doré, 2002; Doré et al, 2008).
228 Northwards increasing peneplanation of the Nyk High (Lundin & Doré, 2002, their Fig. 10)
229 is in all likelihood another expression of Middle Miocene compression.
230

231 While the structural evolution of the palaeo-Vema Dome is comparatively well understood
232 thanks to 3D seismic coverage and wells 6706/11-1 (Vema Dome) and 6707/10-1 (Nyk
233 High), the development of the Hel Graben remains less well understood. In particular,
234 structural geometries of strata in the Hel Graben, the hanging wall to the Nyk High, are
235 unusual.

236
237 The Naglfar Dome (Fig. 1) is the only mid-Cenozoic dome on the mid-Norwegian margin
238 with a present day pronounced bathymetric expression, possibly indicating late movement,
239 but more probably a function of Neogene sediment starvation. Like the Vema Dome, the
240 Naglfar Dome is interpreted to have been inverted in Middle Miocene time (Doré et al,
241 2008). The Hvitvies (6706/6-1) exploration well on the Naglfar Dome in Hel Graben was
242 targeted on a “stripy” seismic succession, interpreted based on reflective character to be the
243 Santonian-Early Campanian Nise Formation. However, seismic tie into the Hel Graben is
244 very difficult, if even possible. Initial reports by the operator (Esso) suggested that the Nise
245 Formation had been penetrated, but biostratigraphic dating by the Norwegian Petroleum
246 Directorate reveals that the well did not penetrate deeper than the Selandian (Williams &
247 Magnus, 2010). Due to the considerable difference in biostratigraphic dating, the Hvitveis
248 well has been re-dated numerous times, more than any other Norwegian well. However, a
249 Paleocene age at TD now appears undisputable (Williams, 2013). IKU shallow borehole
250 6707/04-U-01 on the Naglfar Dome encountered Lower Eocene cemented ash beds lying
251 unconformably beneath the Upper Pliocene/Pleistocene sequence (Mørk et al., 2001). This
252 corroborates our proposal that the Hel Graben collapsed in Paleocene time and contains an
253 unusually thick Paleocene succession.

254
255 The evolution of the area is illustrated by a series of maps and profiles. Structural mapping at
256 Campanian level (top Nise Formation) in the Vema-Nyk area illustrates the present day
257 structure (Fig. 4). Draping of isopachs on the structure map demonstrates the structural-
258 stratigraphic development through time. The Maastrichtian isopach draped over the
259 Campanian structure map (Fig. 5A) brings out the location of the latest Cretaceous palaeo-
260 Vema Dome (the southern end of the Vema-Nyk Anticline). Draping by the Paleocene
261 isochore (Fig. 5 B) shows infill in the collapsed Hel Graben, and draping of the Neogene
262 isopach (Fig. 5C) reveals the location of the present day Vema Dome, c 9 km further west of
263 the palaeo-dome.

264
265 The evolution is also well expressed by an E-W seismic profile across the Vema Dome – Nyk
266 High (Fig. 6). Flattening at the Base Cenozoic unconformity brings out the Late Cretaceous
267 palaeo-Vema Dome (Fig. 6B), and flattening at near top Oligocene level reveals Paleogene
268 infill above the Base Cenozoic unconformity (Fig. 6C), while the present day profile reveals
269 the Middle Miocene inversion.

270
271 The collapse of the western flank of the Vema-Nyk Anticline is illustrated by a NW-SE
272 profile across the Nyk High and southeastern Hel Graben (Fig. 7). A most revealing aspect of
273 this profile is that the unconformity can be followed down the degraded Nyk High fault scarp
274 to at least c 4.5-5 seconds two-way-time depth. This unconformity is correlated with the Late
275 Paleocene unconformity penetrated by exploration well 6706/11-1 (Vema Dome), where the
276 hiatus spans the Early Paleocene and Late Maastrichtian. Notably, the “stripy” strata in Hel
277 Graben are not rotated down against the Nyk High fault system and signs of a syn-rift wedge
278 expanding towards the fault system are lacking (Fig. 8). Rather, the “stripy” strata in Hel
279 Graben thin toward and onlap upwards against the unconformity bounding the Nyk High
280 scarp, resembling geometries typical of collapse features. Strata onlapping the unconformity

281 are clearly Paleocene and younger in age, as the 6706/6-1 well demonstrates (Williams &
282 Magnus, 2010). The Nise Formation and older strata are not imaged in Hel Graben.
283

284 **Discussion**

285 The northern mid-Norwegian margin experienced a series of significant Late Cretaceous and
286 Cenozoic deformational events, spatially overprinting one another. Following Early
287 Cretaceous hyperextension (Lundin & Doré, 2011), the northern part of the basin chain
288 became subject to Late Cretaceous compression. The Vøring basin deformation is not
289 isolated, and can be regarded as a southerly outpost of the more significant contractional
290 structuring observed around the incipient Barents Sea plate boundary to the north. These
291 movements include the principal phase in the development of the Senja Ridge and Veslemøy
292 High in the southwestern Barents Sea, both structural highs resulting from Late Cretaceous
293 inversion and shale diapirism with a suspected strike-slip component. (Riis et al. 1986;
294 Gabrielsen et al. 1990). Farther north, Svalbard was emergent through the entire Late
295 Cretaceous, with erosion apparently increasing northwards across the archipelago (Steel &
296 Worsley, 1984). This curious anomaly at a time of major Mesozoic marine flooding is likely
297 to further represent constriction at the incipient plate boundary. Prior to Early Eocene break-
298 up, Svalbard lay adjacent to the Wandel Sea Basin of northeast Greenland, where small
299 isolated sedimentary basins underwent folding and thrusting in the Late Cretaceous and Early
300 Paleocene (Manby & Lyberis, 2000; Håkansson & Schack-Pedersen, 2001). These
301 compressional movements along the Barents-Greenland margin are usually viewed as
302 resulting from strike-slip, a precursor to the development of a dextral shear margin in the
303 western Barents Sea in the Paleogene (e.g. Håkansson & Schack-Pedersen, 2001), although
304 others regard the compression as orthogonal to the incipient plate boundary (e.g. Manby &
305 Lyberis, 2000).

306
307 Maastrichtian-Paleocene inversion of part of the Vigrid Syncline is documented above. This
308 event inverted the Santonian-Campanian Nise sandstone fairway in the axis of the Vigrid
309 Syncline. The Nise Formation can be linked to a provenance off NE Greenland such as the
310 Danmarkshavn Ridge and to the northwestern Barents Sea margin, both of which underwent
311 uplift in the Late Cretaceous. Erosion to form this voluminous turbidite deposit, at a time of
312 extremely high eustatic sea level, is indicative of active tectonics. Hence, onset of inversion
313 within the Cretaceous basin chain can be inferred back to the Santonian-Campanian at least.
314 As noted, the Vigrid Syncline is not a classic thermal sag response to preceding rifting and it
315 is tempting to suggest that this large fold also may have a compressional origin. However, the
316 difficulty in proposing a compressional origin for this feature lies in the biostratigraphically
317 dated succession in the Gjallar Ridge.

318
319 Three main observations have led to the interpretation of Late Cretaceous extension on the
320 west flank of the Gjallar Ridge (e.g. Lundin & Doré, 1997; Ren et al, 2003, Gernigon et al,
321 2004). These are: 1) onlapping/pinch-out of the post-Late Turonian strata in the Vigrid
322 Syncline against the east flank of the Gjallar Ridge, 2) clear extensional fault blocks on the
323 west flank of the Gjallar Ridge, offsetting a “stripy” seismic succession, and 3) Upper
324 Cretaceous age dating of strata in the 6704/12-1 well on the Gjallar Ridge. A cause-effect
325 relationship is often implied between the Upper Cretaceous-Paleocene onlaps against the east
326 flank of the Gjallar Ridge and the extension on the west side.
327

328 Regardless of model, the “stripy” succession in the fault blocks along the west flank of the
329 Gjallar Ridge have been correlated on seismic character alone. This is arguably analogous to
330 the earlier work in the Hel Graben correlating the Nise Sandstone with the “stripy”
331 succession (e.g. Ren et al, 2004), which was later shown by the 6706/6-1 well to be of
332 Paleocene age. Hence we raise the possibility that the “stripy” succession in the Gjallar Ridge
333 fault blocks may similarly be Paleocene.

334

335 It is unclear if the Late Cretaceous inversion was continuous or episodic. Onlap relationships
336 of Turonian-Paleocene strata in the Vigrid Syncline against the eastern flank of the Gjallar
337 Ridge (e.g. Lundin & Dore, 1997; Ren et al, 2003) reveal that the syncline succession locally
338 coalesces to a single point. This single point onlap suggests that the Gjallar Ridge was
339 actively rising during deposition of the Turonian-Paleocene succession in the Vigrid
340 Syncline. Notably, the Maastrichtian-Paleocene sedimentary fill of the Vigrid Syncline
341 overlapped in time with the rise of the Vema-Nyk Anticline and the associated development
342 and fill of the Någrind Syncline (Fig. 3). Therefore, a conceivable scenario is: a)
343 compressional buckling of the Vøring Basin in Late Turonian time with the development of
344 the Vigrid Syncline, b) continued inversion of the Danmarkshavn Ridge off NE Greenland
345 (and off the greater Svalbard area) during Santonian-Campanian, and c) rise of the Vema-
346 Nyk Anticline in Maastrichtian-Paleocene time. Thus a picture is emerging of semi-
347 continuous inversion of a formerly hyperextended rift basin, with the focus of inversion
348 shifting within the basin.

349

350 We speculate that the Gjallar Ridge predominantly was extended in the Paleocene and that
351 extension along the western flank of the Gjallar Ridge linked with Paleocene extension along
352 the Nyk High via the Rym Fault Zone relay structure. The style of deformation changes from
353 a faulted flexure along the Rym Fault Zone, to a clearly faulted hinge in the Vema Dome
354 area, to the highly degraded collapsed scarp along the central and northern Nyk High (and
355 further north along the western side of the Utrøst Ridge). This change of deformation
356 probably represents progressively more collapse to the north and could relate to changes
357 associated with trap door-style downfaulting of Hel Graben. It is clear from the line of break-
358 up (Fig. 2) that the Paleocene extension cut across the pre-existing Cretaceous basin. Not
359 surprisingly, the suggested distribution of Paleocene extension mimics the line of break-up.

360

361 The dramatic collapse along the Nyk High and the Rym Fault Zone resembles caldera
362 collapse geometries (Branney, 1995). Indeed it has previously been proposed that Hel Graben
363 represents a large Paleocene caldera (Lundin et al, 2002). If formed by a caldera eruption the
364 size of the Hel Graben would be indicative of an acidic caldera (ref). ODP site 642 on the
365 Vøring Marginal High, located c. 150 km southwest of the Hel Graben, drilled through an
366 upper series of tholeiitic flows before drilling 142 m of dacitic rocks, including ignimbrites
367 (Eldholm et al., 1989). Based on the flow chemistry, Taylor and Morton (1989) concluded
368 that these rocks were sourced from a shallow magma chamber and were derived from partial
369 melting of the continental crust. The ignimbrites prove that acidic explosive eruptions took
370 place in outer Vøring margin prior to extrusion of tholeiitic lava associated with break-up.
371 The age of the dacitic sequence in ODP 642, derived from two single-crystal ^{40}Ar - ^{39}Ar dates,
372 is 54.3 \pm 0.5 and 55.6 \pm 2.0 Ma (Late Paleocene-earliest Eocene) (Sinton et al., 1998).
373 Eldholm et al. (1989) suggested that the lower series dacites correspond to the North Sea Sele
374 Fm, which contains graded ashes of both silicic and basaltic composition (Knox & Morton,
375 1988).

376

377 While a caldera explanation for the Hel Graben collapse is speculative, the unusual style of
378 vertical collapse is more definite. The caldera concept is only one of several potential causes
379 of such collapse. What collapse features have in common, however, is the removal of a
380 volume of material at depth, be it molten rock in a magma chamber, dissolution or
381 withdrawal of halite, melting of ice, mine shaft collapse, or deflation of a balloon in analog
382 experiments (e.g. Marti et al., 1994; Branney, 1995; Ge & Jackson, 1998; Roche et al., 2000;
383 Troll et al., 2002). Removal of crustal volume beneath the Hel Graben could be tied to a
384 number of causes. Caldera eruption is one, magma-withdrawal, or crustal delamination
385 during break-up are other possibilities. The nature of the mid-Norwegian marginal high
386 remains unresolved, and this enigmatic feature has been interpreted to be made up of
387 transitional crust and is thus a candidate for laterally displaced magmatic rocks.
388

389 We have argued in an earlier paper (Lundin & Doré, 2011) that the deformation events
390 described above were possible because the area was prone to deformation, as a consequence
391 of lithospheric weakening by Early Cretaceous hyperextension. Hyperextension is suggested
392 to lead to a significant reduction of lithospheric strength due to: a) thinning of the crust by a
393 total stretching factor of 3-4 or more, and b) associated partial serpentinization of the upper
394 mantle. Weakening related to hyperextension and associated partial serpentinization of the
395 upper mantle has been demonstrated numerically (Lundin et al, 2012; Wienecke et al, 2012).
396 Late Cretaceous compressional deformation started c 20-40 m.y. prior to break-up of the NE
397 Atlantic and the last compressional deformation postdated break-up by c 40 m.y. Thus,
398 whatever the cause of the compressional events, they unlikely can be attributed to the break-
399 up process.
400

401 In principle, the compressional deformation could be thin-skinned and constrained to
402 the crust, i.e. separated from the mantle by partially serpentinized uppermost mantle.
403 However, such a solution provides a problem in balancing an undeformed underlying
404 mantle from a deformed overlying crust. Alternatively, the entire lithosphere is
405 deformed (cf Cloetingh & Burov, 2010), and if so, that would suggest that such
406 lithospheric weakening is long-lived (c 115 m.y.) and that the lithospheric strength does not
407 increase as rapidly as suggested by e.g. Close et al (2009).
408
409
410
411
412
413
414

415 **Implications for the Petroleum System**

416
417 Widely spaced fault blocks dismembered by large-heave low-angle faults are to be
418 expected from hyperextension (c.f. Osmundsen & Ebbing, 2008; Peron-Pindivic and
419 Manatschal, 2009). Therefore, a patchy distribution of the Upper Jurassic source rock is
420 likely, since it would have been part of the pre-rift succession. More importantly, the
421 source rock would have already been buried deeply already during the Early to mid-
422 Cretaceous, causing maturation of the source rock and expulsion of hydrocarbons before
423 or close in time to the deposition of Upper Cretaceous reservoirs, and certainly well
424 before trap development related to Late Cenozoic compressional inversion (e.g. Naglfar
425 and Vema Domes) (Doré et al, 1999). A minor late gas charge, probably from leaner

426 source rocks postdating the Jurassic, is found in the Nise Formation within nearby
427 inversion-related traps (Snefrid and Haklang discoveries).

428

429 The proposed weakness related to hyperextension allowed the mid-Norwegian margin to
430 deform readily. Latest Turonian development of the Vigrid Syncline generated a fairway
431 for deposition of the Santonian-Campanian Nise Formation turbidites, (Fig 1). Inversion
432 by the Vema-Nyk Anticline probably blocked this fairway and diverted the subsequent
433 Maastrichtian Springar Formation turbidites, mainly to the outer (western) flank of the
434 fold.

435

436 The Maastrichtian-Early Paleocene Vema-Nyk Anticline may have formed early enough
437 to receive charge from an Upper Jurassic source rock, but regardless of whether
438 hydrocarbons were originally trapped in this large structure, the fold was breached by
439 faulting and erosion in Late Paleocene time (Fig. 6c). Much of the hydrocarbon charge
440 will probably have been lost to the surface. The Aasta Hansteen (Luva) Field, a c 1.5
441 TCF gas accumulation in the Nise Formation on the Nyk High associated with a well-
442 defined seismic flat spot (Goodall et al. 2002), may represent remnant charge of more
443 likely a late gas charge.

444

445 The previously unrecognized collapse of Hel Graben led to misidentification of the
446 reservoir drilled on the Naglfar Dome by well 6706/6-1 (Fig. 8). However, regardless of
447 the age of the reservoir, the main challenge of this prospect still relates to the late
448 development of the structure.

449

450

451 **Conclusions**

452

453 1) The mid-Norwegian margin was originally part of a hyperextended Early Cretaceous basin
454 chain. The hyperextension caused a significant and arguably long-lived (c 115 m.y) reduction
455 of the lithospheric strength, making the area prone to multiple phases of compressional
456 deformation. The long-lived weakness of the margin, here related to crustal hyperextension
457 and partial serpentinization of the mantle, suggests that lithospheric strengthening does not
458 occur as rapidly as some authors propose.

459

460

461 2) The interplay between Cretaceous and Cenozoic compressional phases, and intervening
462 pre-breakup extension, resulted in a complex and variable pattern of vertical motions across
463 the northern Vøring Basin

464

465 3) Late Cretaceous compressional inversion may have been initiated in Cenomanian-
466 Turonian time, but no later than intra-Maastrichtian time. The compression created or
467 enhanced the characteristic syncline-anticline architecture of the Vøring Basin. It is
468 suggested that features such as the Vigrid and Någrind Synclines, most often assumed to
469 represent passive post-extensional subsidence features were a consequence of this
470 compressional deformation.

471

- 472 4) Prior to latest Cretaceous inversion, the Vigrid Syncline continued northwards, at least
473 through the Hel Graben but possibly also outboard of the Utrøst Ridge.
474
- 475 5) The latest phase of Late Cretaceous inversion occurred in the Vema-Nyk-Hel area. A
476 major updomed area, the Vema-Nyk Anticline, started forming in Maastrichtian time and
477 inverted the palaeo-Vigrid Syncline.
478
- 479 6) Subsequent pre-breakup extension was mainly of Paleocene age and was focused on the
480 anticlines. Major collapse occurred on the western flank of the Vema-Nyk Anticline forming
481 the Hel Graben, an enigmatic structure lacking usual rift geometries. Anticline collapse also
482 took place along the western flank of the Gjallar Ridge and in the Fenris Graben. Less
483 pronounced extension occurred along the Utgard High/Fles Fault Complex.
484
- 485 7) After Early Eocene break up, the northern Vøring Basin was imprinted by further mild
486 compression, modifying the Nyk High and Hel Graben area and forming the Vema and
487 Naglfar Domes.
488

489 **Acknowledgements**

490 The ideas presented here date back almost a decade and several Statoil colleagues working on
491 production licenses 217 and 218 were consulted at the time. We are indebted to their
492 comments. We express our gratitude to Statoil and former partners in production licenses 217
493 and 218, BP and Conoco-Phillips. The views presented here are our own and do not
494 necessarily represent a company view.

495 **References**

496 BLYSTAD, P., BREKKE, H., FÆRSETH, R.B., LARSEN, B.T., SKOGSEID, J. & TØRUDBAKKEN, B.
497 1995. Structural elements of the Norwegian continental shelf: *Norwegian Petroleum*
498 *Directorate Bulletin No. 8*.

499
500 BRANNEY, M.J. 1995. Downsag and extension at calderas: new perspectives on collapse
501 geometries from ice-melt, mining, and volcanic collapse. *Bulletin of Volcanology*, **57**, 303-
502 318.

503
504 BREKKE, H. 2000. The tectonic evolution of the Norwegian Sea continental margin with
505 emphasis on the Vøring and Møre Basins. In: Nøttvedt, A. Et al. (eds) *Dynamics of the*
506 *Norwegian Margin*, Geological Society Special Publication, London, **167**, 327-378.

507
508 BREKKE, H. SJULSTAD, H.I., MAGNUS, C. & WILLIAMS, R.W. 2001. Sedimentary
509 environments offshore Norway – an overview. In: MARTINSEN, O.J. & DREYER, T. (eds),
510 *Sedimentary Environments Offshore Norway – Palaeozoic to Recent*, Norwegian Geological
511 Society Special Publication **10**, 7-37.

512
513 CHALMERS, J.A., AND PULVERTAFT, T.C.R., 2001, Development of the continental
514 margins of the Labrador Sea: A review, in Wilson, R.C.L., et al., eds., *Nonvolcanic*

515 *rifting of continental margins: A comparison of evidence from land and sea*: London,
516 Geological Society of London Special Publications
517 **187**, p. 77–105.
518

519 CLOETINGH, S. & BUROV, E. 2010. Lithospheric folding and sedimentary basin evolution: a
520 review and analysis of formation mechanism. *Basin Research*, **23**, 257-290, doi:
521 10.1111/j.1365-2117.2010.00490x
522

523 CLOSE, D.I., WATTS, A.B. & STAGG, H.M.J., 2009, A marine geophysical study of the Wilkes
524 Land rifted continental margin, Antarctica. *Geophysical Journal International*, **177**, 430-450,
525 doi:10.1111/j-1365-246x.2008.0466.x
526

527 DORÉ, A.G., LUNDIN, E.R., JENSEN, L.N., BIRKELAND, Ø., ELIASSEN, P.E., AND FICHLER, C.,
528 1999, Principal tectonic events in the evolution of the northwest European Atlantic margin, *in*
529 FLEET, A.J. AND BOLDY, S.A.R. (eds), *Petroleum Geology of Northwest Europe: Proceedings*
530 *of the 5th Conference*, Geol. Soc. London, p. 41-61.

531 DORÉ, A.G., LUNDIN, E.R., KUSZNIR, N.J. AND PASCAL, C. 2008, Potential mechanisms for
532 the genesis of Cenozoic domal structures on the NE Atlantic margin: pros and cons and some
533 new ideas, *in* JOHNSON, H. ET AL. (eds), *The Nature and Origin of Compression in Passive*
534 *Margins*: Geological Society, London, Special Publications **306**, p. 1-26, doi:
535 10.1144/SP306.5.
536

537 GABRIELSEN, R.H., FÆRSETH, R.R., JENSEN, L.N., KALHEIM, J.E. & RIIS, F. 1990.
538 Structural elements of the Norwegian continental shelf. Part 1, The Barents Sea region.
539 Norwegian Petroleum Directorate Bulletin, 6, 33 p.
540

541 GE, H. & JACKSON, M.P.A. 1998. Physical modelling of structures formed by salt withdrawal:
542 Implications for deformation caused by salt dissolution. *Bulletin of American*
543 *Association of Petroleum Geologists*, **82**, 228-250.
544

545 GERNIGON, L., RINGENBACH, J.-C., PLANKE, S., AND LE GALL, B. 2004. Deep structures and
546 breakup along volcanic rifted margins: insights from integrated studies along the outer
547 Vøring Basin (Norway). *Marine and Petroleum Geology*, **21**, 363-372,
548 doi:10.1016/j.marpetgeo.2004.01.005
549

550 GOODALL, I., WESTLAKE, I., VAGLE, G.B., MUNDAL, I. & MULCAHY, M. 2002,
551 Resistivity Image Data, Vøring Basin, Offshore Norway, *in* Geological Applications of Well
552 Logs, M. Lovell and N. Parkinson, eds.: AAPG Methods in Exploration No. 13, p. 143-159
553

554 HAMANN, N.E., WHITTAKER, R. & STEMMERIK, L. 2005. Geological development of the
555 Northeast Greenland Shelf. In: DORÉ, A.G & VINING, B.A. (eds) *Petroleum Geology: North-*
556 *West Europe and Global Perspectives—Proceedings of the 6th Petroleum Geology*
557 *Conference*, Geol. Soc. London, 887–902.
558

559 HANSEN, J.W., BAKKE, S., FANAVOLL, S. ET AL. 1992. *Shallow drilling Nordland*
560 *VI and VII 1991—Main Report*. IKU report, **23**.1594.00/02/92.
561

562 HAQ, B.U., HARDENBOL, J. & VAIL, P. 1988. Mesozoic and Cenozoic chronostratigraphy and
563 cycles of sea-level change. In: Wilgus, C.K. et al (eds), *Sea-Level Changes: An Integrated*

564 *Approach*. Society of Economic Paleontologists and Mineralogists, Special Publication **42**,
565 71-108.

566

567 HÅKONSSON, E. & SCHACK PEDERSEN, S.A. 2001. The Wandel Hav Strike-Slip
568 Mobile Belt - A Mesozoic plate boundary in North Greenland. *Bulletin of the Geological*
569 *Society of Denmark*, 48, 149-158.

570

571 JOHNSON, H., RITCHIE, J. D., HITCHEN, K., MCINROY, D. B. & KIMBELL, G. S.
572 2005. Aspects of the Cenozoic deformational history of the Northeast Faroe–Shetland Basin,
573 Wyville-Thomson Ridge and Hatton Bank areas. In: DORÉ, A. G. & VINING, B. A. (eds)
574 *Petroleum Geology: North-West Europe and Global Perspectives*. Proceedings of the 6th
575 Petroleum Geology Conference. Geological Society, London, 993–1008.

576

577 KITILSEN, J.E., OLSEN, R.R., MARTEN, R.F., HANSEN, E.K. & HOLLINGSWORTH, R.R.1999.
578 The first deepwater well in Norway and its implications for the Upper Cretaceous Play,
579 Vøring Basin. *Geological Society, London, Petroleum Geology Conference series 1999*, **5**,
580 275-280, doi: 10.1144/0050275.

581

582 LOUDEN, K.E. & CHIAN, D. 1999. The deep structure of non-volcanic rifted
583 continental margins, *Phil. Trans. R. Soc. Lond.* **357**, 767- 805.

584

585 LUNDIN, E.R. & DORÉ, A.G. 1997. A tectonic model for the Norwegian passive margin with
586 implications for the NE Atlantic: Early Cretaceous to break-up. *Journal of the Geological*
587 *Society, London*, **154**, 545-550.

588

589 LUNDIN, E.R. & DORÉ, A.G. 2002. Mid-Cenozoic post-breakup deformation in the “passive”
590 margins bordering the Norwegian- Greenland Sea. *Marine & Petroleum Geology*, **19**, 79-93.

591

592 LUNDIN, E.R., RØNNING, K., DORÉ, A.G. & OLESEN, O. 2002. Hel Graben, Vøring Basin,
593 Norway – a possible major cauldron? The 25th Nordic Geological Winter Meeting,
594 Reykjavik, Jan 6-9.

595

596 LUNDIN, E.R. & DORÉ, A.G. 2011. Hyperextension, serpentinitization, and weakening: A new
597 paradigm for rifted margin compressional deformation. *Geology*, **39**, 347–350, doi:
598 10.1130/G31499.1.

599

600 LUNDIN, E.R., DORÉ, A.G. AND WIENECKE, S., 2012. The hyperextended mid-Norwegian
601 margin - implications for exploration. Third Central & North Atlantic Conjugate Margin
602 Conference, Trinity College, Dublin, Aug 22-24, p. **XX-YY**.

603

604 MAHER, H.D., JR., 2001, Manifestations of the Cretaceous high Arctic large igneous province
605 in Svalbard: *Journal of Geology*, **109**, p. 91–104, doi: 10.1086/317960.

606

607 MANBY, G. & LYBERIS, N., 2000. Pre-ocean opening of the Northwestern Atlantic
608 margin: evidence from eastern North Greenland. *Journal of the Geological Society*,
609 *London*, 157, 707-710.

610

611 MARTI, J., ABLAY, G.J., REDSHAW, L.T. & SPARKS, R.S.J. 1994. Experimental studies of
612 collapse calderas. *Journal of the Geological Society, London*, **151**, 919-929.

613
614 MORTON, A.C., WHITHAM, A.G., FANNING, C.M. & CLAOUÉ-LONG, J. 2005. The role of East
615 Greenland as a source of sediments to the Vøring Basin during the late Cretaceous. *Onshore-*
616 *Offshore Relationships of the North Atlantic Margins*, NPF Special Publication **12**, 83.110.
617
618 MORTON, A.C. & GRANT, S. 1998. Cretaceous depositional systems in the Norwegian Sea:
619 Heavy mineral constraints. *Bulletin of the American Association of Petroleum Geologists*, **82**,
620 274-290.
621
622 MØRK, M.B.E., LEITH, D.A. & FANAVOLL, S. 2001. Origin of carbonate-cemented beds on the
623 Naglfar Dome, Vøring Basin, Norwegian Sea. *Marine and Petroleum Geology*, **18**, 223-234.
624
625 OSMUNDSEN, P.T., EBBING, J., 2008. Styles of extension offshore mid-Norway and
626 implications for mechanisms of crustal thinning at passive margins. *Tectonics*, v. 27,
627 TC6016, doi:10.1029/2007TC002242.
628
629 PÉRON-PINDIVIC, G., AND MANATSCHAL, G., 2009, The final rifting evolution at deep magma
630 poor passive margins from Iberia-Newfoundland: A new point of view: *Int. Jour. Earth*
631 *Sci.*, v. 98, p. 1581-1597, doi: 10.1007/s00531-008-0337-9.
632
633 PÉREZ-GUSSINYÉ, M., AND RESTON, T.J., 2001, Rheological evolution during extension at
634 non-volcanic rifted margins: Onset of serpentinization and development of detachments
635 leading to continental break-up: *Journal of Geophysical Research*, **106**, 3961–3975, doi:
636 10.1029/2000JB900325.
637
638 PLANKE, S., ALVESTAD, E. & ELDHOLM, O. 1999. Seismic characteristics of basaltic extrusive
639 rocks, *The Leading Edge*, **March**, 342-348.
640
641 REN, S., FALEIDE, J.I., ELDHOLM, O., SKOGSEID, J. & GRADSTEIN, F. 2003. Late Cretaceous –
642 Paleocene tectonic evolution of the NW Vøring Basin. *Marine and Petroleum Geology*, **20**,
643 177-206.
644
645 RIIS, F., VOLLSET, J. & SAND, M., 1986. Tectonic Development of the Western Margin of
646 the Barents Sea and Adjacent Areas. AAPG Special Volumes, M 40: Future
647 Petroleum Provinces of the World, 661 - 675.
648
649 ROBERTS, D. G., THOMPSON, M., MITCHENER, B., HOSSACK, J., CARMICHAEL, S. &
650 BJØRNSETH, H.-M. 1999. Palaeozoic to Tertiary rift and basin dynamics: mid-Norway to the
651 Bay of Biscay – a new context for hydrocarbon prospectivity in the deep water frontier. In:
652 FLEET, A. J. & BOLDY, S. A. R. (eds) *Petroleum Geology of Northwest Europe: Proceedings*
653 *of the 5th Conference*. Geological Society, London, 7–40.
654
655 ROCHE, O., DRUITT, T.H. & MERLE, O. 2000. Experimental study of caldera formation.
656 *Journal of Geophysical Research*, **105**, B1, 395-416.
657
658 SHIPILOV, E.V. & KARYAKIN, Y.V. 2011. The Barents Sea Magmatic Province:
659 Geological–Geophysical Evidence and New ⁴⁰Ar/³⁹Ar Dates. *Doklady Earth Sciences*, **439**,
660 Part 1, 955–960.
661

662 SKOGSEID, J., PLANKE, S., FALEIDE, J.I., PEDERSEN, T., ELDHOLM, O. & NEVERDAL, F. 2000.
663 NE Atlantic continental rifting and volcanic margin formation. In: NØTTVEDT, A. et al (eds),
664 *Dynamics of the Norwegian Margin*. Geological Society, London, Special Publications, **167**,
665 295-326.

666

667 SKOGSIED, J. & ELDHOLM, O. 1988. Early Cainozoic evolution of the Norwegian volcanic
668 passive margin and the formation of marginal highs. In: Morton, A.C. & Parson, L.M. (eds).
669 *Early Tertiary Volcanism and the Opening of the NE Atlantic*, Geological Society Special
670 Publication, **39**, 49-56.

671

672 SKOGSIED, J. & ELDHOLM, O. 1989. Vøring continental margin: seismic interpretation,
673 stratigraphy and vertical movements. In: Eldholm, O., Thiede, J., and Taylor, E. (eds)
674 *Proceedings of the Ocean Drilling Program, Scientific Results* **104**, College Station, TX,
675 993-1030.

676

677 STEEL, R. J. & WORSLEY, D. 1984. Svalbard's post-Caledonian strata: an atlas of
678 sedimentational patterns and palaeogeographic evolution. In: SPENCER, A. M. et al.
679 (eds) *Petroleum Geology of the North European Margin*. Norwegian Petroleum
680 Society/Graham & Trotman, London, 109-135

681

682 TROLL, V.R., WALTER, T.R. & SCHMINCKE, H.-U. 2002. Cyclic caldera collapse: Piston or
683 piecemeal subsidence? Field and experimental evidence. *Geology*, **30**, 135-138.

684

685 TSIKALAS, F., FALEIDE, J.I., ELDHOLM, O. & WILSON, J. 2005. Conjugate mid-Norway and
686 NE Greenland continental margins. In: DORÉ, A.G. & VINING B.A. (eds) *Petroleum Geology:
687 North-West Europe and Global Perspectives—Proceedings of the 6th Petroleum Geology
688 Conference*, 785–801.

689

690 TUITT, A, UNDERHILL, J.R., RITCHIE, J.D., JOHNSON, H. & HITCHEN, K. 2010. Timing,
691 controls and consequences of compression in the Rockall-Faroe area of the NE Atlantic
692 Margin. *Geological Society, London, Petroleum Geology Conference series*. **7**, 963-977, doi:
693 10.1144/0070963.

694

695 WALKER, I., BERRY, K., BRUCE, J.R. BYSTØL, L. & SNOW, J.H. 1997. Structural modelling of
696 regional depth profiles in the Vøring Basin: implications for the structural and stratigraphic
697 development of the Norwegian passive margin. *Journal of the Geological Society, London*,
698 **154**, 537-544.

699

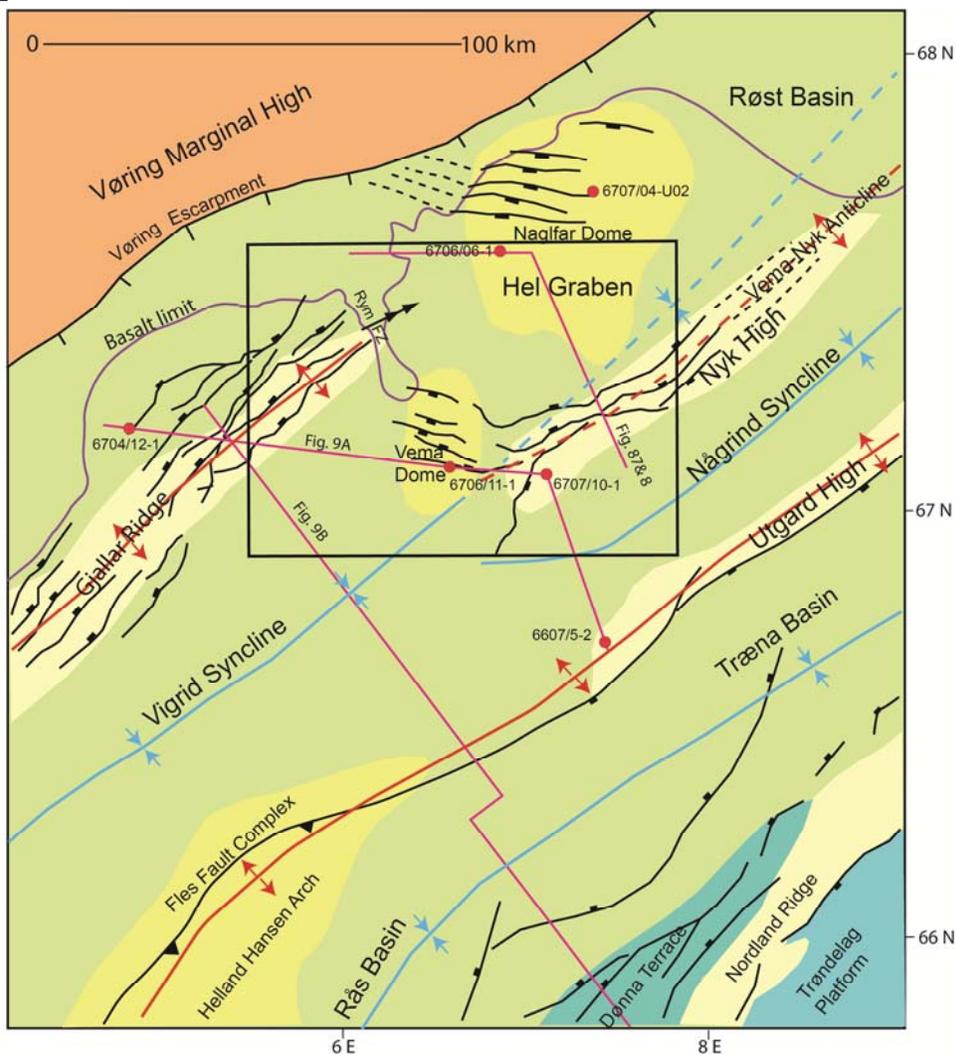
700 WIENECKE, S. AND LUNDIN, E.R. 2012. A short notice on the importance of the Youngs
701 modulus on the interpretation of crustal strength. EGU meeting, Vienna 22-27.

702

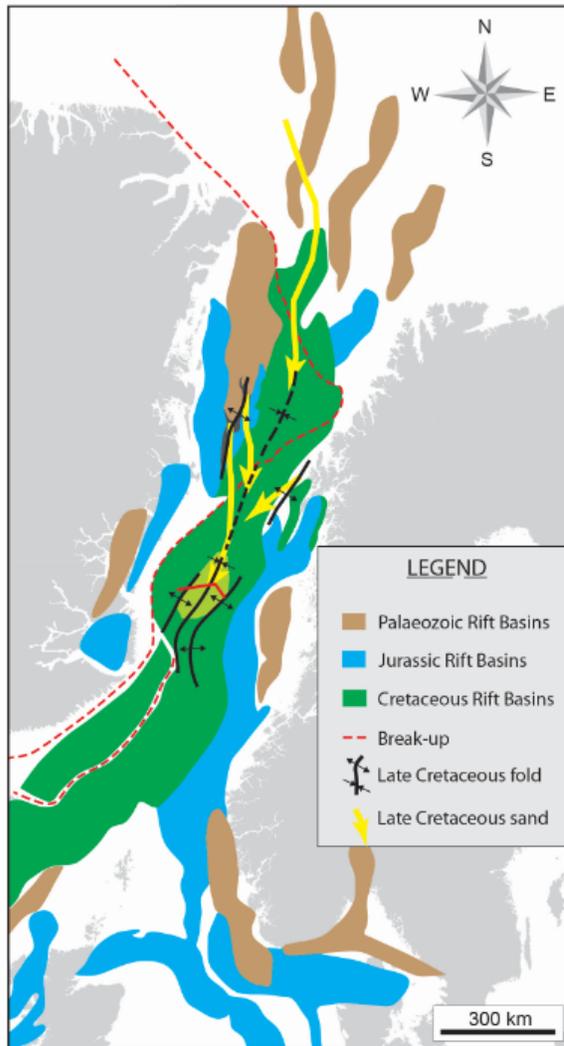
703 WILLIAMS, R.W. & MAGNUS, C. 2010. Four key wells of the northern Vøring
704 Basin: Grønøy High, Gjallar Ridge, Hel Graben and Nyk High. *29th Nordic Geological
705 Winter Winter Meeting*, Oslo, Jan 11-13, Norwegian Geological Society, 212.

706

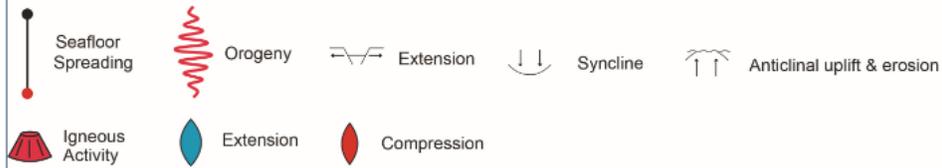
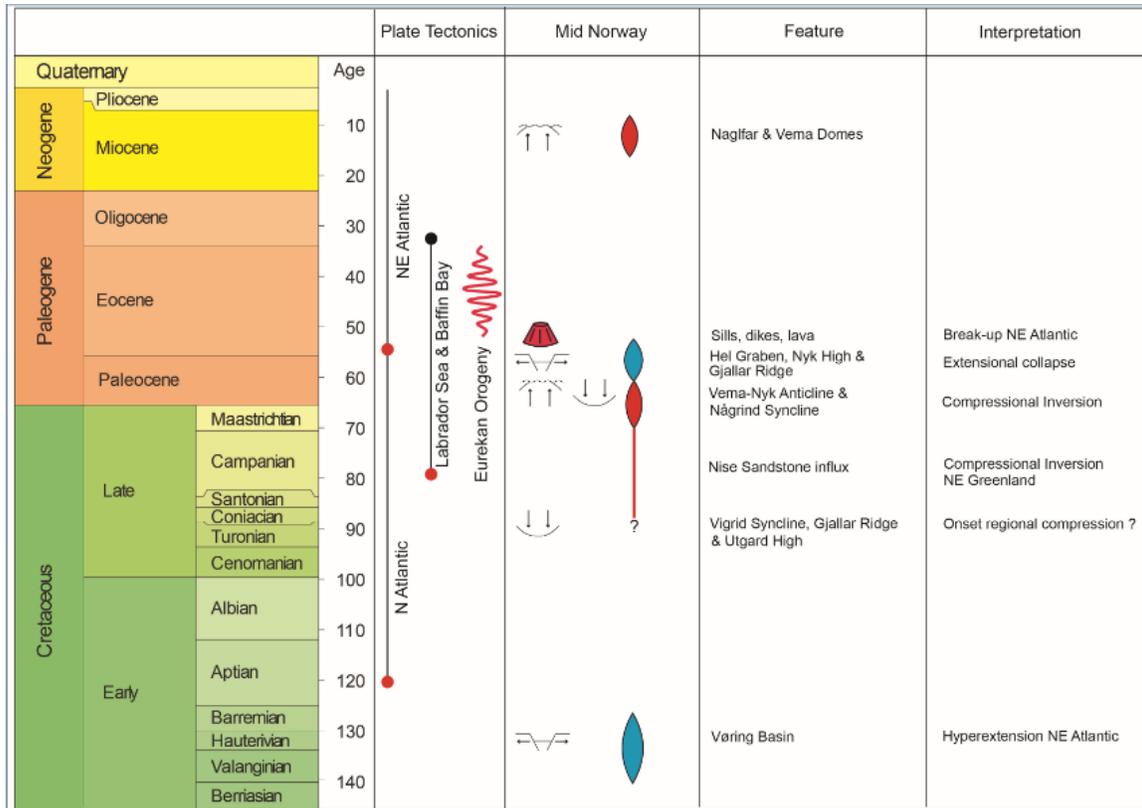
707 **Figure captions**



708
709
710 Fig. 1 Structural features map of northern mid-Norwegian margin (after Blystad et al, 1995).
711 Inset box marks area of figures 4 and 5. Profiles are labelled with figure number.
712
713

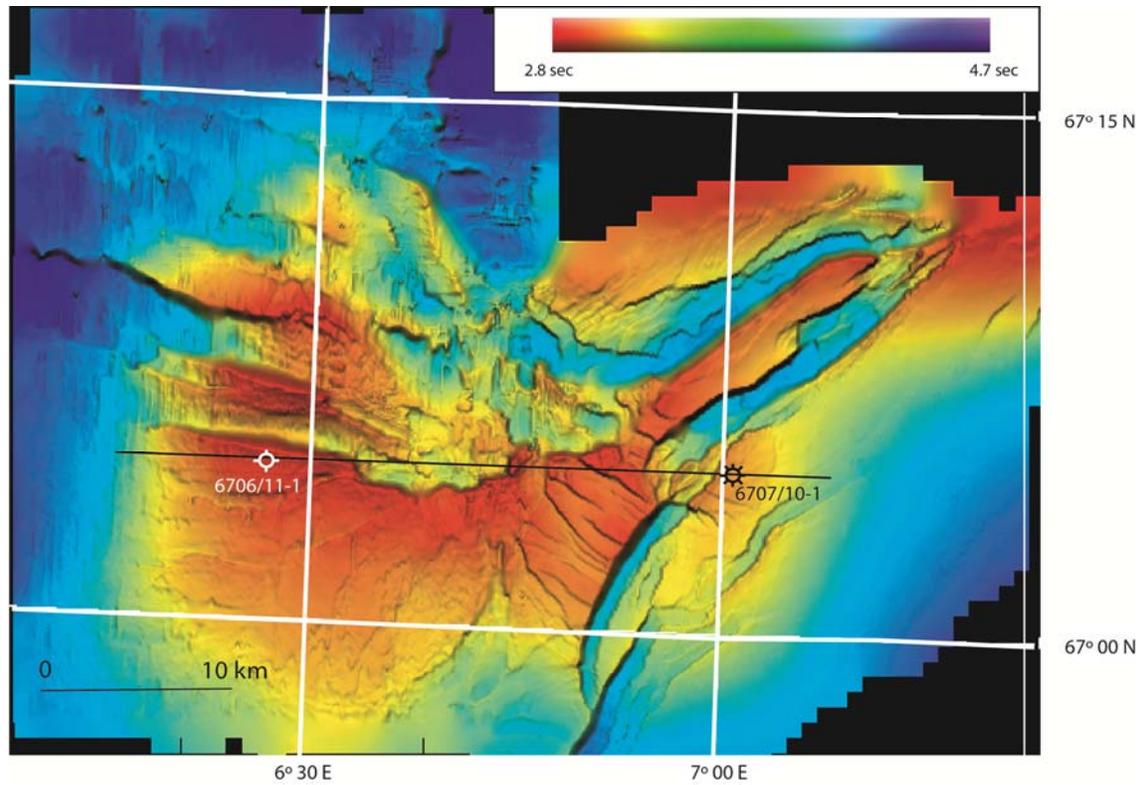


714
 715 Fig. 2 Pre-breakup plate reconstruction to 53 Ma, illustrating how younger rifts overprint
 716 older at an oblique angle and how erosional products from inverted areas were shed into the
 717 palaeo Vigrid Syncline. Red profile is Fig 9b.
 718

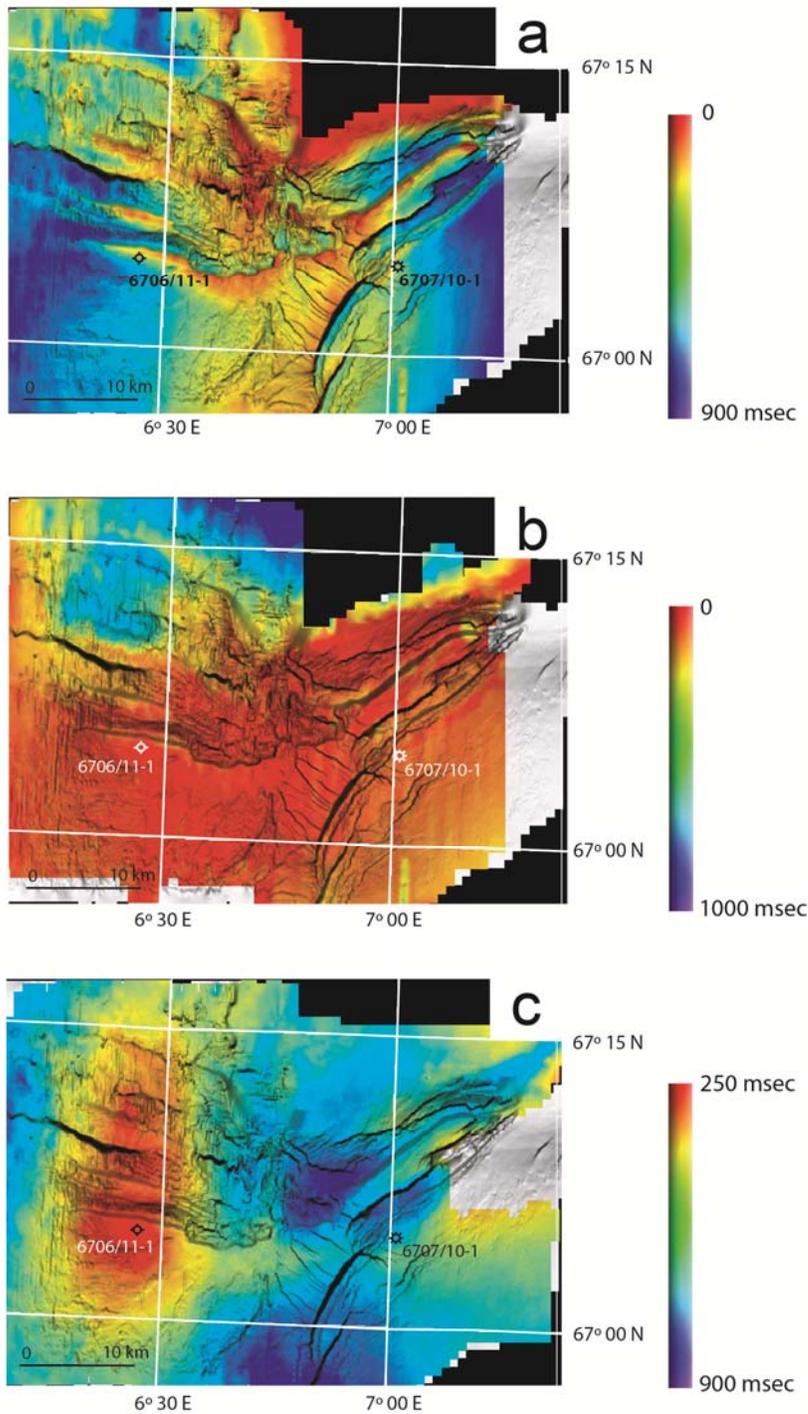


719
720
721

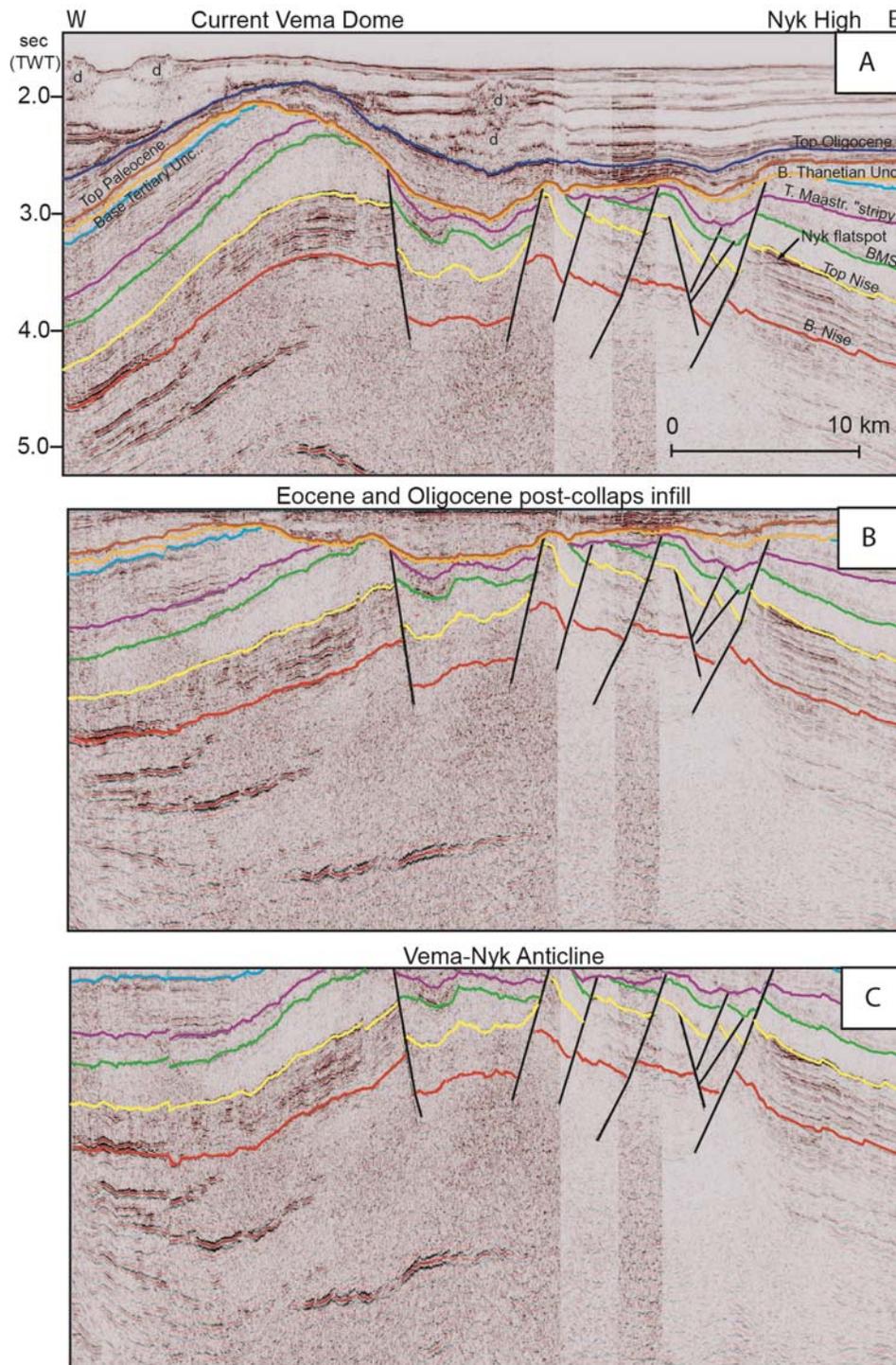
Fig. 3 Tectonic events chart.



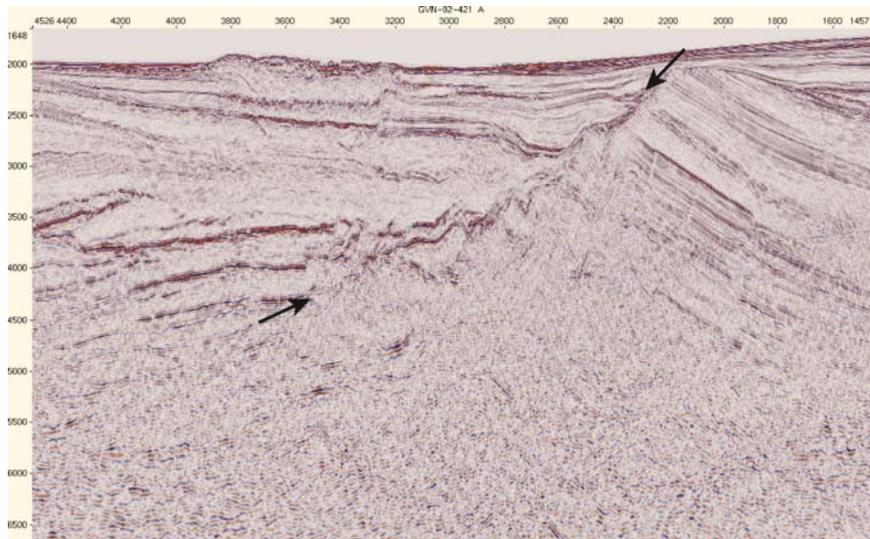
722
 723 Fig. 4. Shaded relief structural map of the present day Vema Dome- Nyk High area at top
 724 Campanian level (Nise Formation) level.
 725



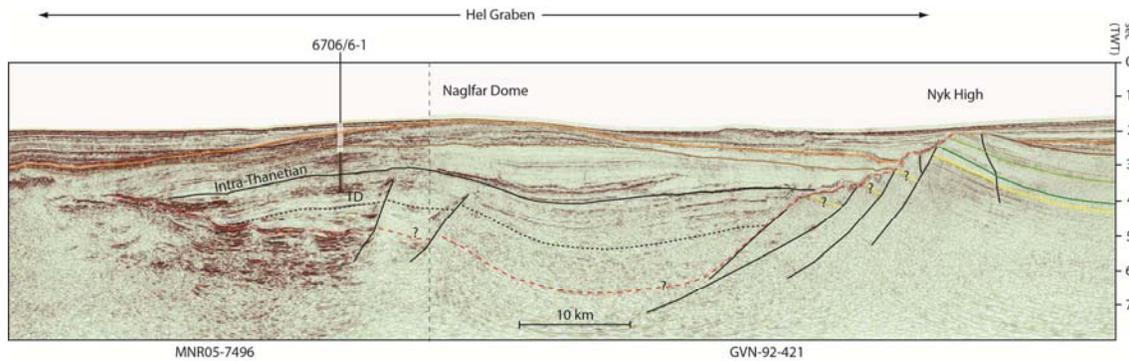
726
 727 Fig 5. Shaded relief maps, with isochore maps draped over the Campanian structure map of
 728 Fig. 4. Colours indicate isochore thickness in relationship to the palaeo-Vema Dome
 729 structure. a) Maastrichtian isochore demonstrating erosional truncation above the palaeo-
 730 Vema Dome, b) Paleocene isochore illustrating collapse into Hel Graben, c) Neogene
 731 isochore illustrating inversion of the current dome.
 732



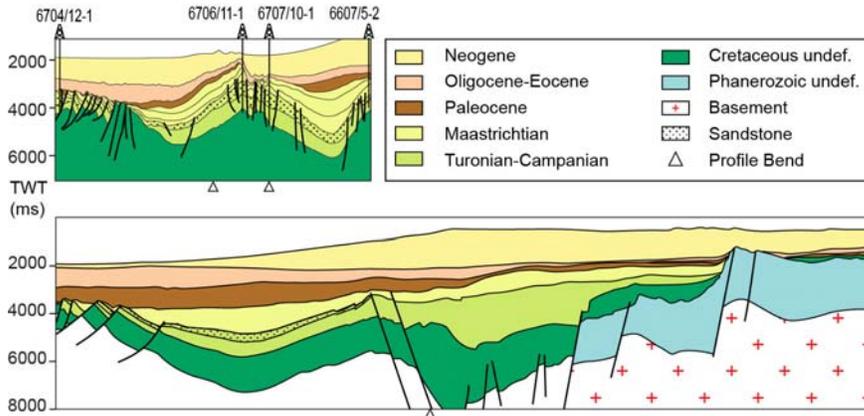
733
 734 Fig. 6. E-W seismic profile across the Vema Dome and Nyk High revealing main structural
 735 stages. A: Present day, revealing the Middle Miocene Vema Dome. B: Flattened on top
 736 Oligocene, revealing Paleocene-Eocene infill after Late Paleocene collapse along the Nyk
 737 High extensional system. C: Flattened on the Base Cenozoic unconformity, revealing the
 738 Vema-Nyk Anticline.
 739



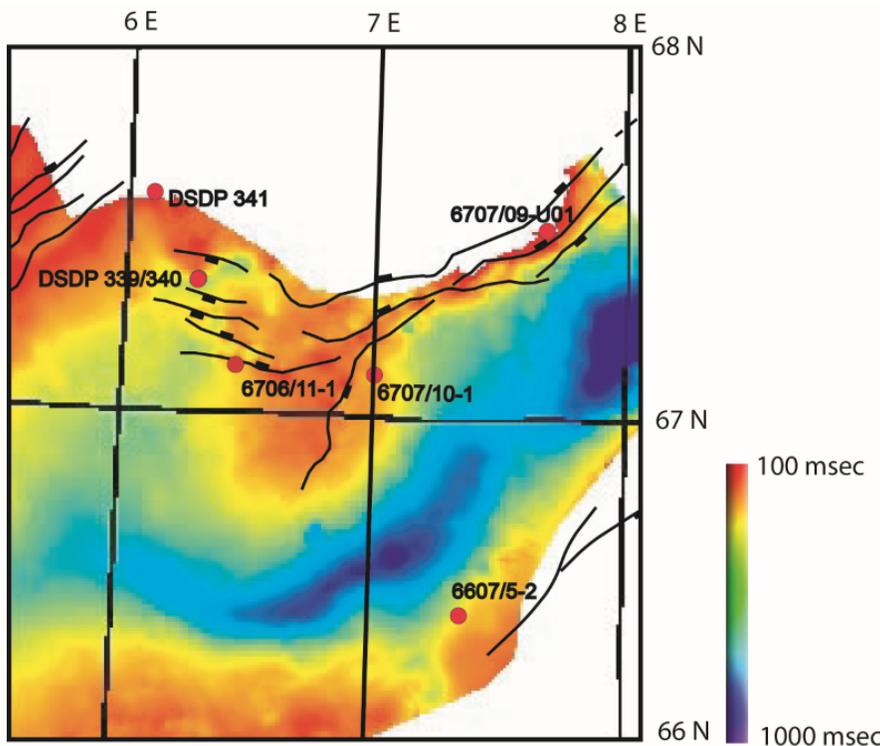
740
 741 Fig. 7 NW-SE oriented seismic profile GVN92-421 across the Nyk High and eastern side of
 742 Hel Graben (for location see Fig. 1), illustrating the collapsed western flank of the Nyk High
 743 (the former Vema-Nyk Anticline). The Paleocene unconformity (marked by arrows)
 744 bounding the degraded fault scarp can be followed to at least 4.5 sec TWT. Note how the
 745 strata in Hel Graben lap on upwards against the unconformity.
 746



747
 748 Fig. 8 NW-SE oriented seismic profile across Nyk High and southeastern Hel Graben, tying
 749 to well 6706/6-1 (for location see Fig. 1). The well terminated in Selandian age strata, which
 750 can be seen to onlap the fault scarp. The upper white part of the well had returns of cuttings
 751 to seabed while the lower gray shaded part was sampled.
 752



753
 754 Fig. 9A) Geoseismic profile between the Gjallar Ridge (6704/12-1), Vema Dome (6706/11-1),
 755 Nyk High (6707/10-1) and Utgard High (6607/5-2) wells. The section illustrates that the
 756 Santonian-Early Campanian Nise Fm (stippled) was deposited in an unstructured saucer-
 757 shaped basin, which subsequently was inverted by the rise of the Vema-Nyk Anticline, also
 758 forming the Någrind Syncline. Note that the western half of the section lies south of the Hel
 759 Graben and, therefore, was unaffected by its collapse structuring. 9B) The Turonian-
 760 Maastrichtian Vigrid Syncline (left half of profile), the Utgard High and the Rås Basin. For
 761 location see Fig 1. After Lundin & Doré (2011).
 762



763
 764 Fig. 10. Simplified Maastrichtian isochore map (TWT). The lack of Maastrichtian strata in
 765 Hel Graben is a function of difficulty of mapping below the base Thanetian unconformity.
 766 The map reveals the onset of folding of the Vema-Nyk Anticline and the Någrind Syncline.